3D finite element simulation of equal channel angular pressing with different material models

Patil Basavaraj V

Rungta College of Engineering and Technology, Raipur-492099, India.

***Abstract*— Ultra-fine grained materials have been widely investigated due to their improved mechanical properties such as high strength and ductility. Various techniques have been developed to obtain such mechanical properties. Among those, the Equal Channel Angular Pressing (ECAP) process is one of the effective methods of obtaining materials with high strength and toughness. Finite element method is one of the important approaches to understand the deformation occurring in the ECAP process. Material model plays very important role in modeling the process. In the present work simulation ECAP was presented for different material models namely, elastic, perfectly plastic and strain hardening. Three channel angles 90, 105 and 120 degree were considered for analysis. The general purpose software, ABAQUS/Standard was used for this purpose. Effect of different material models on strain, strain inhomogeneity and load required for extrusion has been presented.**

Index Terms— Sever Plastic Deformation, Metal Forming, Equal Channel Angular Pressing (ECAP), Finite Element Analysis (FEA), ABAQUS

I. INTRODUCTION

Fabrication of bulk materials with ultra-fine grain sizes has attracted much attention in the last decade because of the recognition that these materials exhibit numerous attractive properties including relatively high strength at ambient temperatures and a potential for utilization in superplastic forming operations at elevated temperatures. Different techniques have been used to introduce large plastic strains into bulk metals, such as Equal Channel Angular Pressing (ECAP) [1]-[2], Accumulative Roll Bonding [3], [4] and [5], Repetitive Corrugation and Straightening [5]-[6], Constrained Groove Pressing (CGP)[7], and Constrained Groove Rolling (CGR) [4].

Ultra-fine grained (UFG) metallic materials have many desirable properties such as high strength and toughness. Some metals exhibit superplastic behavior. The ultra-fine grained metals with grain sizes in the range from 0.3 to 1 micron provide a reasonable compromise between high strength and satisfactory ductility that is attractive for structural applications. Because of these properties the fabrication of bulk materials has attracted much attention in the last decade. Techniques for producing ultra-fine grained metals have special scientific and commercial interest. Conventional methods for producing fine-grained structure in bulk materials are thermo mechanical treatments, which combine deformation and recrystallisation, and solid-state phase transformations such as in steels and titanium alloys. The grain size produced by these conventional methods is greater than 1μm. Severe plastic deformation (SPD) techniques for producing UFG have a number of advantages. First, one can produce bulk products (sheets, rods) economically, which can be used for mechanical testing. Secondly, no residual porosity is found in the parts produced. Thirdly, it is possible to use electron diffraction microscopy for more complete investigation of the structure of UFG materials. Hence interest is increasing on the use of SPD for the production of bulk ultra-fine grained materials.

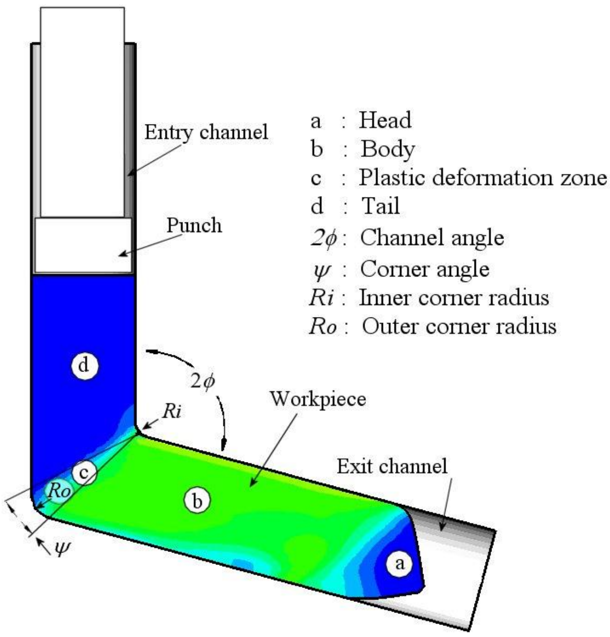

Fig. 1 Principle of ECAP process

Segal *et al.* [8] proposed and demonstrated the concept of Equal Channel Angular Pressing, subjecting large volumes of material to simple shear in order to modify their microstructure and enhance properties. The most highly cited work on SPD that has spawned the development of ECAP and related techniques for producing ultra-fine grain materials is that of Valiev *et al.* [9]-[10]. Other SPD methods include Cyclic Extrusion-Compression (CEC) [11], torsion under hydrostatic pressure [12], Accumulative Roll Bonding (ARB) process [13], Equal Channel Angular Drawing (ECAD) [14]-[15], Repetitive Corrugation and Straightening (RCS)[5]-[6], Constrained Groove Pressing (CGP) [7], and Constrained Groove Rolling (CGR) [4].

II. EQUAL CHANNEL ANGULAR PRESSING

Many researchers have shown that ultra-fine grains can be obtained after ECAP deformation in materials, such as pure copper [16], pure aluminium [17]-[18], Al-Mg alloys [19]-[20], and other Al alloys [21].

Although several techniques are now available for the fabrication of ultra-fine grained materials, the most attractive and versatile procedure is ECAP where a workpiece is pressed through a die, which consists of channels of equal cross-sectional area. The general principle of ECAP is illustrated in Fig. 1. The workpiece is pressed through a die with two channels of equal cross section, intersecting at an angle (channel angle, 2ϕ) ranging between 90° and 120°, having corner angle of ψ. The workpiece under deformation can be divided into four zones namely (a) head (the front of the workpiece) (b) body (c) plastic deformation zone and (d) tail (the undeformed portion at the end of the workpiece). Since the workpiece undergoes deformation without change in shape, it can be pressed several times to obtain desired accumulation of plastic strain. During plastic deformation of metals by this process the grain size reduces to sub-micron level and mechanical properties improve. Grain size and mechanical properties thus developed can be controlled by proper selection of ECAP process parameters.

III. FINITE ELEMENT ANALYSIS

The Finite Element Method (FEM) is a powerful numerical tool initially formed to solve linear applied mechanics problems. It is now developed to solve any kind of non-linear problems (Zienkiewicz and Taylor [22] , Belytschko *et al.*[23]). Due to the advent in computer technology the FEM can now be applied to any complicated large problems. ECAP is a very complex process with non-linearity arising from geometry, material behavior and contact between die and workpiece. Literature survey showed that FEM had been applied to study ECAP since the 1997. Several authors reported the work on die geometry, friction, back pressure and material models using plane strain 2D approximation. Commercially available softwares like ABAQUS, MARC, DEFORM etc. were successfully used to model the process. A brief survey of the work is presented in the following sections.

1) Material Models

Simple shear plastic deformation behavior of polycarbonate (PC) plates due to ECAP process was modeled by Sue *et al.* [24]. The study revealed that ECAP process is effective in producing a high degree of simple shear plastic deformation across the extruded polycarbonate plates. The high degree of plastic deformation due to ECAP induces a high level of nearly uniform molecular orientation across the extruded PC plate.

The most uniform flow can be obtained in ECAP of a strain-hardening material having low strain-rate sensitivity in tooling with a sharp inner corner radius [25]. The ECAP of materials with other constitutive behaviors or a rounded corner die will produce inhomogeneity.

Lee *et al.* [26] investigated the plastic deformation during ECAP of an aluminum alloy composite containing particles and porosities. Based on the distribution of the maximum principal stress in the workpiece, Weibull fracture probability was obtained for particle sizes and particle-coating layer materials. The probability agreed well with the trend of more susceptible failure of brittle coating layer than particle without an inter-phase in metal matrix composites.

Zairi *et al.* [27] investigated the plastic response of a polymer during ECAP at room temperature. Aour *et al.* [28] showed the influence of various geometrical parameters and material properties on polymers.

Figueiredo *et al.* [29] studied ECAP of flow-softening materials. Flow-softening rate affects the intensity of shear localization. The deformation zone, that is usually concentrated around a fixed shear plane during processing of perfect plastic or strain hardening materials, splits into two parts and its position varies cyclically during the process, leading to oscillations in the punch load during the processing.

A. MATERIAL BEHAVIOR

Mechanism of plasticity in metals has been well identified as slip due to motion of dislocations in crystals. As a result, the plastic deformation is closely associated with shear deformation, no volume change occurs due to plastic deformation, and plastic behavior in tension and compression are almost identical. All these characteristics are common to most of the metals.

Microscopically, engineering materials are inhomogeneous, and not all elements yield at the same time. The transition from elasticity to plasticity thus takes place in a homogeneous fashion and this is why a smooth transition in an overall stress-strain curve is observed. However, macroscopically, these materials can be considered as homogeneous, whose element yields at the elastic limit and deforms in the way an overall stress-strain response indicate.

1) Stress-Strain Relation in Elastic Range

For a homogeneous, continuous and isotropic solid, the elastic stress strain relations are given by the following equations

$$\varepsilon_{11} = \frac{1}{E}[\sigma_{11} - \upsilon(\sigma_{22} + \sigma_{33})] \qquad (1)$$

$$\varepsilon_{22} = \frac{1}{E}[\sigma_{22} - \upsilon(\sigma_{33} + \sigma_{11})] \qquad (2)$$

$$\varepsilon_{33} = \frac{1}{E}[\sigma_{33} - \upsilon(\sigma_{11} + \sigma_{22})] \qquad (3)$$

$$\gamma_{12} = 2\varepsilon_{12} = \frac{1}{G}\sigma_{12} \qquad (4)$$

$$\gamma_{23} = 2\varepsilon_{23} = \frac{1}{G}\sigma_{23} \qquad (5)$$

$$\gamma_{31} = 2\varepsilon_{31} = \frac{1}{G}\sigma_{31} \qquad (6)$$

where ε_{ij} is strain, γ_{ij} is shear strain and σ_{ij} stress in the direction *i* on the plane *j*. E is the Young's modulus of the material, υ is the Poisson's ratio and G is the rigidity or shear modulus. Combining all the equations (1.) to (6.) the generalised stress-strain relation in the elastic range can be written as

$$\varepsilon_{ij} = \frac{S_{ij}}{2G} + \delta_{ij}\frac{(1-2\upsilon)\sigma_m}{E} \qquad (7)$$

where S_{ij} is deviotoric stress in the direction *i* on the plane *j*, σ_m is hydrostatic stress and δ_{ij} is Kronecker delta. In the elastic range the hydrostatic pressure cannot be neglected because it causes an elastic volume change. In this case the hydrostatic stress and strain are connected by the following equation:

$$\varepsilon_{kk} = \frac{(1-2\upsilon)\sigma_{kk}}{E} \qquad (8)$$

In elastic range the following 11 equations are to be solved simultaneously:

Equilibrium equations	$\frac{\partial \sigma_{ij}}{\partial x_i} = 0$	3 No.s
Stress-strain relations	$\varepsilon_{ij} = \frac{S_{ij}}{2G} + \delta_{ij}\frac{(1-2\upsilon)\sigma_m}{E}$	6 No.s
Hydrostatic Stress-strain relation	$\varepsilon_{kk} = \frac{(1-2\upsilon)\sigma_{kk}}{E}$	1 No.
Yield criterion: von-Mises	$k_f = \sqrt{\frac{3}{2}S_{ij}S_{ij}}$	1 No.
Total		11 No.s

2) Von-Mises Yield Criterion

The von-Mises Criterion, also known as the maximum distortion energy criterion, octahedral shear stress theory or Maxwell-

Huber-Hencky-von Mises theory, is often used to estimate the yield of ductile materials.

The von-Mises criterion states that failure occurs when the energy of distortion reaches the same energy for yield/failure in uniaxial tension. Mathematically, this is expressed as,

$$k_f = \sqrt{\frac{3}{2} S_{ij} S_{ij}} \quad (9)$$

or

$$k_f = \sqrt{\frac{1}{2}\left[(\sigma_{11}-\sigma_{22})+(\sigma_{22}-\sigma_{33})+(\sigma_{33}-\sigma_{11})\right]+3\left[\sigma_{12}^2+\sigma_{23}^2+\sigma_{31}^2\right]} \quad (10)$$

where k_f is the uniaxial flow stress and S_{ij} is the stress deviator tensor.

3) Stress-Strain Relation in Plastic and Elasto-Plastic range

The first approach to plastic stress-strain relation was suggested by Saint-Venant in 1970, who proposed that the principal axes of strain increment coincided with the principal stress axes. The general three-dimensional equations relating the increments of total strain to the stress deviations were given by Levy in 1871 and independently by von-Mises in 1913. These equations are known as the Levy-Mises equations. These equations are

$$\frac{d\varepsilon_{11}}{S_{11}} = \frac{d\varepsilon_{22}}{S_{22}} = \frac{d\varepsilon_{33}}{S_{33}} = \frac{d\varepsilon_{12}}{S_{12}} = \frac{d\varepsilon_{23}}{S_{23}} = \frac{d\varepsilon_{31}}{S_{31}} = d\lambda \quad (11)$$

or

$$\dot{\varepsilon}_{ij} = \dot{\lambda} S_{ij} \quad (12)$$

where S_{ij} is the stress deviator tensor and $\dot{\lambda}$ is a function of the material constant and strain rate. In these equations the total strain increments are assumed to be equal to the plastic strain increments, the elastic strains being ignored. Thus these equations can only be applied to problems of large plastic flow and cannot be used in the elasto- plastic range. The generalization of Eq. (12) to include both elastic and plastic components of strain is due to Prandtl and Reuss and are known as Prandtl-Reuss equations in which it is assumed that the total strain in sum of elastic and plastic strain, i.e.

$$\varepsilon_{total} = \varepsilon_{elastic} + \varepsilon_{plastic} \quad (13)$$

and hence the stress strain relation in elasto-plastic range is given by

$$\dot{\varepsilon}_{ij} = \frac{\dot{S}_{ij}}{2G} + \dot{\varepsilon} S_{ij} \quad (14)$$

In plastic range the following 10 equations are to be solved simultaneously:

Equilibrium equations	$\frac{\partial \sigma_{ij}}{\partial x_i} = 0$	3 No.s
Continuity equation	$\dot{\varepsilon} = 0$	1 No.s
Levy-Mises equations	$\dot{\varepsilon}_{ij} = \dot{\lambda} S_{ij}$	6 No.s
Total		10 No.s

B. SOLUTION TO THE PROBLEM

Advancements in computer technology have spurred the rapid development of a powerful modern numerical technique, Finite Element Method (FEM), for obtaining solutions of almost any complex engineering problems by computer. Incremental inelastic analysis of virtually any boundary-value problems can be solved today by the FEM. This development has greatly benefited the field of metal forming that it has provided the classical theory of plasticity with newer concepts and wider applications.

C. SOFTWARE

The ABAQUS (version 6.5-1) finite element software was chosen to perform all the simulations conducted throughout these investigations. It is a general-purpose software that has been successfully implemented to solve a wide variety of problems in the areas of structural analysis and other disciplines of mechanical engineering. Additionally, ABAQUS allows certain interactions among multiple engineering disciplines such as thermal-electrical and thermal-structural coupled-field problems. There is a wide range of elements that are available in ABAQUS. This extensive element library provides the user with a powerful set of tools for solving problems of different areas.

In ABAQUS there are two solvers, ABAQUS/Standard and ABAQUS/Explicit. ABAQUS/Standard is a general-purpose finite element module and uses implicit time integration. For each step equilibrium has to be obtained. It analyses many types of problems, for example static, dynamic and thermal. ABAQUS/Explicit is an explicit dynamics finite element module.

In ABAQUS an interactive, graphical environment called the Complete Abaqus Environment (CAE) is used for modeling, managing and monitoring analysis and visualizing results. In the CAE the different parts used in an analysis are created. Parts can also be imported from other CAD programs. The parts are assigned material properties and assembled into a model. After configuring the analysis procedure and applying loads and boundary conditions, the model is ready to be meshed. After the model is completely defined, an input file containing all the model information is generated and submitted for processing.

1) Choosing Elements for Plasticity Problem

Incompressibility imposed by plasticity in metals limits the type of elements that can be used for elasto-plastic simulations. This limitation arises from the kinematic constraint imposed on element behavior namely constraint of constant volume at the element integration point. In some cases, this actually makes the element over-constrained. Elements that cannot resolve this constraint suffer from volumetric locking, that is, overly stiff response. Fully integrated, second-order, solid elements are very susceptible to volumetric locking in elastic-plastic simulations. The ABAQUS fully integrated, first-order, solid elements do not suffer from volumetric locking because ABAQUS actually uses a constant volume strain in these elements. Reduced integration, solid elements have fewer integration points at which the incompressibility constraints must be satisfied. Therefore, they are not over-constrained and can be used for most elastic-plastic simulations. In simulations, with plastic strains exceeding 20-40% second-order, reduced integration elements may be used and with fine meshes.

2) Choosing Element for Rigid Bodies

In ABAQUS a rigid body is a collection of nodes and elements whose motion is governed by the motion of a single node, known as the rigid body reference node. The shape of the rigid body is defined as an analytical surface or discrete rigid body. The analytical surface is obtained by revolving or extruding a 2D geometric profile. A discrete rigid body is obtained by meshing the component with nodes and elements. The shape of the rigid body remains constant during an analysis. The body can undergo large rigid body motions. Computation of mass and inertia for a discrete rigid body can be based upon contribution from its elements. It can also be assigned specifically.

Boundary conditions governing the motion of a rigid body are applied to the rigid body reference node. Contact and nodal connections are used for interaction of rigid bodies and deformable elements. Rigid bodies are typically used to model very stiff components. These components may be fixed or undergoing large rigid body motions. In forming analyses, rigid bodies are an excellent choice for modeling components such as punches, dies, rollers etc. The computational efficiency provided by rigid bodies is the primary reason for choosing them above deformable elements. Element-level computations are avoided and relatively small effort is required to update the motion of the nodes and assemble concentrated/distributed loads.

3) Material Models

The material library in ABAQUS allows most engineering materials to be modeled, including metals, plastics, rubbers, foams, composites, granular soils, rocks, and plain and reinforced concrete. This section only discusses metal plasticity.

The yield and inelastic flow of a metal at relatively low temperatures, where creep effects are not important and loading is relatively monotonic, can typically be described with the classical metal plasticity. Standard von-Mises or Hill yield surfaces with associated plastic flow are implemented in ABAQUS for this purpose. Perfect plasticity and isotropic hardening definitions are both available in the classical metal plasticity models. The von-Mises and Hill yield surfaces assume that yielding of the metal is independent of the equivalent pressure stress. The von-Mises yield surface is used to define isotropic yielding. It is defined by giving the value of the uniaxial yield stress as a function of uniaxial equivalent plastic strain, temperature, and/or field variables on the data lines or by defining the yield stress in user subroutines.

The Hill yield surface allows anisotropic yielding to be modeled. A reference yield stress must be given, and the user must define a set of yield ratios. ABAQUS provides two types of work hardening: perfect plasticity and isotropic hardening. In perfect plasticity the yield stress does not change with plastic strain while in isotropic hardening means the yield surface changes size uniformly in all directions such that the yield stress increases (or decreases) in all stress directions as plastic straining occurs.

If isotropic hardening is defined, the yield stress can be defined in tabular form or described through user subroutines. If the tabular form is used, the yield stress must be given as a tabular function of plastic strain and, if required, of temperature and/or other predefined field variables. The yield stress at a given state is simply interpolated from this table of data, and it remains constant for plastic strains exceeding the last value given as tabular data. Associated plastic flow is used. Therefore, as the material yields, the inelastic deformation rate is in the direction of the normal to the yield surface (the plastic deformation is volume invariant). ABAQUS optionally allows for plastic dissipation to result in the heating of a material. The option is typically used in the simulation of bulk metal forming or high-speed manufacturing processes involving large amounts of inelastic strain where the heating of the material caused by its deformation is an important effect. The option is applicable only to adiabatic thermal-stress analysis or fully coupled temperature-displacement analysis. Only the von-Mises yield surface can be used in an adiabatic analysis.

When defining plasticity data in ABAQUS, the user must provide true stress and true strain. ABAQUS requires these values to interpret the data in the input file correctly. ABAQUS approximates the smooth stress-strain behavior of the material with a series of straight lines joining the given data points. Any number of points can be used to approximate the actual material behavior; therefore, it is possible to use a very close approximation of the actual material behavior. The material data defines the true yield stress of the material as a function of true plastic strain. The first piece of data given defines the initial yield stress of the material and, therefore, should have a plastic strain value of zero.

4) Non-linear Analysis

A non-linear structural problem is one in which the structure's stiffness changes as it deforms. In non-linear analysis, the stiffness matrix of the structure has to be assembled and inverted many times during the course of the analysis, making it much more expensive to solve than a linear analysis. Since the response of a non-linear system is not a linear function of the magnitude of the applied load, superposition cannot be applied to obtain the solution. Each load case must be defined and solved as a separate analysis.

a) Boundary non-linearity

This occurs if the boundary conditions change during the analysis. Boundary non-linearity is extremely discontinuous: when contact occurs during a simulation, there is a large and instantaneous change in the response of the structure.

b) Geometric non-linearity

Geometric non-linearity occurs whenever the magnitude of the displacements affects the response of the structure. This may be caused by large deflections or rotations, snap through, initial stresses or load stiffening. If the deflection is small, the analysis can be considered as being approximately linear. However, if the deflections are large, the shape of the structure and hence its stiffness changes. In addition, if the load does not remain perpendicular to the structure, the action of the load on the structure changes significantly. Both of these effects contribute to the non-linear response of the structure. To incorporate the effects of geometric non-linearity in an analysis NLGEOM parameter has to be set to 1 in *STEP option.

c) Material non-linearity

Most metals have a fairly linear stress/strain relationship at low strain values, but at higher strains the material yields, at which point the response becomes non-linear and irreversible.

5) Non-linear Problem and Solution Techniques:

Many algorithms exits for solving non-linear equations. Following three iterative methods are widely used in finite element analysis:

a) Newton-Raphson Method

b) Modified Newton-Raphson Method

c) Quasi-Newton Method

ABAQUS implements the Newton-Raphson method to obtain solutions for non-linear problems. In a non-linear analysis the solution cannot be calculated by solving a single system of equations, as would be done in a linear problem. Instead, the solution is found by applying the specified loads gradually and incrementally working toward the final solution. Therefore, ABAQUS breaks the simulation into a number of *load increments* and finds the approximate equilibrium configuration at the end of each load increment. It often takes ABAQUS several iterations to determine an acceptable solution to a given load increment. The sum of all of the incremental responses is the approximate solution for the non-linear analysis.

It is important to know the terms analysis *STEP*, load *INCREMENT*, and *ITERATION*. The load history for a simulation consists of one or more steps. The analysis *STEP* generally consists of an analysis procedure and loading. Different boundary conditions and analysis procedure options can be specified in each step. An *INCREMENT* is part of a *STEP*. In non-linear analyses the total load applied in a step is broken into smaller increments so that the non-linear solution path can be followed. At the end of each increment the structure is in (approximate) equilibrium. An *ITERATION* is an attempt to find an equilibrium solution in an increment. If the model is not in equilibrium at the end of the iteration, ABAQUS tries another iteration. With every iteration, the solution ABAQUS obtains should be closer to equilibrium; sometimes ABAQUS may need many iterations to obtain an equilibrium solution. When an equilibrium solution has been obtained, the increment is complete.

6) Contact Problem

Metal forming problems involve contact between two or more components. In these problems a force normal to the contacting surfaces acts on the two bodies when they touch each other. If there is friction between the surfaces, shear forces may be created that resist the tangential motion (sliding) of the bodies.

Contact conditions are a special class of discontinuous constraint, because forces are applied only when the two surfaces are in contact. When the two surfaces separate, no constraint is applied. The FE code has to be able to detect when two surfaces are in contact. Then it must apply the required constraints. It must also detect separation of surfaces and enforce subsequent removal of constraints.

The distance separating two surfaces is called the clearance. With zero clearance between the surfaces the contact constraint is applied. There is no limit in the contact formulation on the magnitude of contact pressure that can be transmitted between the surfaces. Separation of surfaces occurs when the contact pressure between them becomes zero or negative. The contact constraint is then removed. This surface interaction behavior, is referred to as "hard" contact.

The change in contact pressure that occurs when a contact condition changes from "open" (a positive clearance) to "closed" (clearance equal to zero) sometimes makes it difficult to complete contact simulations. In contact simulations, ABAQUS should detect contact at a particular point and also calculate sliding between the two contacting surfaces.

The analysis may need to take into account frictional resistance if the two interacting surfaces are rough. Coulomb friction is a common friction model used to describe the interaction of contacting surfaces. The model characterizes the frictional behavior between the surfaces using a coefficient of friction, μ. The product μp, where p is the contact pressure between the two surfaces, gives the limiting frictional shear stress for the contacting surfaces. The contacting surfaces will not slip (slide relative to each other) until the shear stress across their interface equals the limiting frictional shear stress, μp . For most surfaces μ is normally less than unity.

IV. FINITE ELEMENT MODELING OF ECAP

In the present work, a three-dimensional model was considered for the analyses. As mentioned earlier two-dimensional *plane strain* approximation can be used when the thickness of the workpiece is very large and *plane stress* approximation can be used when the thickness is very small. Both *plane strain* and *plane stress* conditions are not applicable for the cylindrical workpiece used in ECAP. *Axi-symmetric* two-dimensional approximation is also not suitable because the axes of the channels intersect at an angle 2ϕ. Only half of the die-workpiece portion was considered for the analyses because of the symmetry about the parting surface.

A. MODELING OF THE WORKPIECE

The workpiece used for analysis was cylindrical in shape with diameter 19.8 mm and length 105 mm. At the entry side filleting of 1 mm x 1 mm was done as shown in Fig. 1**.** Material used for workpiece was Aluminum alloy AA 6101 with flow stress given by $\sigma_0 = 208\varepsilon^{0.25}$. Fig. 2 shows the experimentally obtained flow stress used for analyses. It was assumed that the hardening behavior is isotropic and independent of strain rate and temperature.

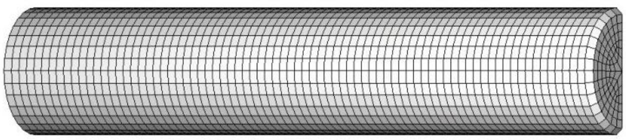

Fig. 1 Meshing of the workpiece used for ECAP

The element used for meshing the workpiece was of the type *continuum (solid) 8 noded* (C3D8) and it is shown in Fig. 3. It has 6 degrees of freedom (three translational and three rotational), namely X, Y, Z, Rx, Ry and Rz. As it uses linear interpolation in each direction it is often called linear element or first-order elements. This element is formulated based on the *Lagrangian* or *material* description. The full *Gaussian quadrature* technique is used to integrate various quantities over the volume of the element as explained in the ABAQUS users manual.

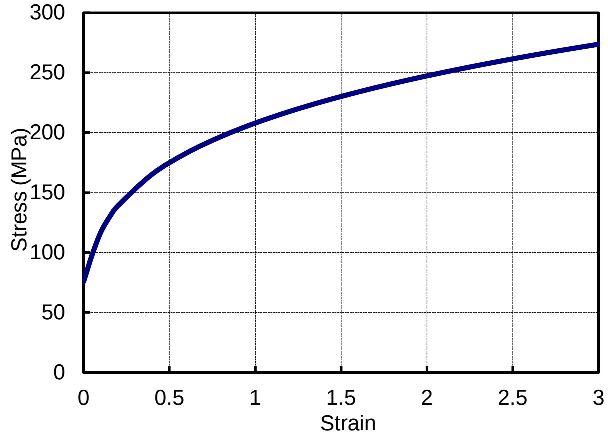

Fig. 2 Stress-Strain curve of AA6101 Aluminum

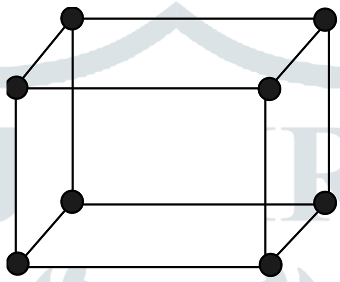

Fig. 3 Eight noded 3D continuum element (C3D8)

B. MODELING OF THE DIE

The die considered for analyses was made of high strength steel (H11). As the steed is very strong compared to the alluminium, the die can be considered as rigid a body with no deformation. Only the inner surface of the channels is important for the purpose of analyses. Hence the die was modeled as rigid surface with the element of type R3D4 as show in Fig. 4. R3D4 is rigid element with 4 nodes. In ABAQUS a rigid body is a collection of nodes and elements whose motion is governed by the motion of a single node, known as the *rigid body reference node*. The motion of a rigid body can be prescribed by applying boundary conditions to the *rigid body reference node*. Rigid bodies, formed by the rigid elements, interact with the rest of the model through nodal connections. Only the *rigid body reference node* has independent degrees of freedom. For R3D4 element the reference node has three translational and three rotational degrees of freedom. Since the element is not deformable, it does not use numerical integration points. There are no element output variables. The only output is the motion of the nodes. The reaction forces and reaction moments are available at the *rigid body reference node*.

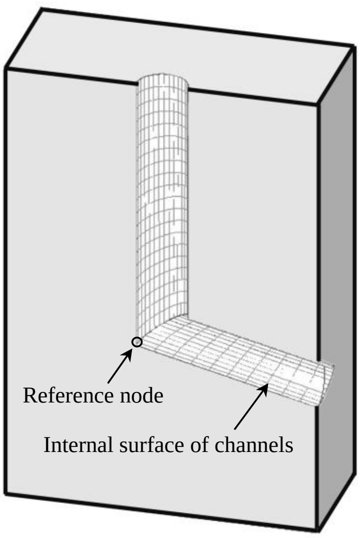

Fig. 4 The die and the internal surface used for meshing

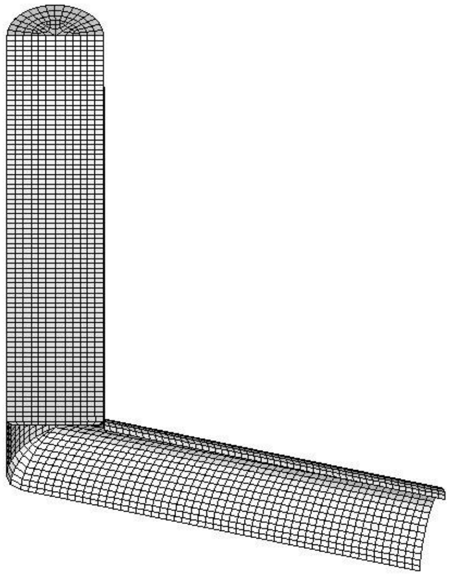

Fig. 5 Meshed assembly of die and workpiece

C. BOUNDARY CONDITIONS

The die and the workpiece were assembled as shown in the Fig. 5. Heat generation due to friction and deformation was ignored. The boundary conditions applied to the model were as follows:

i) Displacement and rotation in x, y and z direction for nodes in of the die were arrested. It was done by arresting all degrees of freedom of *rigid body reference node* corresponding to the die.

ii) As the conditions were symmetric about the parting surface, all the nodes on this surface of the workpiece were constrained in the direction perpendicular to it.

iii) The top surface of the workpiece is in contact with the punch and takes load resulting in the movement of the workpiece. All nodes on the top surface of the workpiece were given displacement in the direction of movement of workpiece.

iv) A contact pair was specified with the die as master and the workpiece as slave.

V. RESULTS AND DISCUSSION

As per the above description CAD models were prepared using ABAQUS/CAE and *input* files were generated using a desktop computer. The *input* files were submitted for simulation to the server through *telnet*.

Processing time required for each simulation varied depending on number of elements in the workpiece and the number of iterations. Initially for modeling the effect of channel angle, number of nodes and elements used for the workpiece was 24062 and 21420 respectively. It took around 1200 iterations to complete the simulation in 86 to 100 hours.

The post processing of the ABAQUS *output database* (.odb) files was done using the desktop computer. Contour plots showing the distribution of equivalent plastic strain (PEEQ in ABAQUS) in various sections was obtained using ABAQUS/CAE. Equivalent plastic strain at the nodes in different zones of the deformed workpiece was taken as output.

This data was used for calculating (i) average equivalent plastic strain in the body of the workpiece (ii) strain inhomogeneity in the body of the workpiece (iii) variation of strain inhomogeneity along the axis of the workpiece and (iv) variation of strain along the radial lines. The reaction force generated at the *rigid body reference node* of the die was taken as output. This data was used for (i) plotting the force v/s stroke graph and (ii) finding the peak pressure required for extrusion. The data obtained from the simulations and their analyses are presented in the following paragraphs.

In case of perfectly elastic material, as expected, workpiece regained its original shape completely and hence there was no plastic strain.

Plastic strain was not observed in head and tail portion of workpiece, both perfectly plastic and strain hardening materials, which is clear from Fig. 2, Fig. 3 and Fig. 4. From these figures it is also clear that the corners are not completely filled in case of strain hardening material. In all the cases there was large amount of variation in strain within the steady state zone. This variation in strain is termed as strain inhomogeneity [30]. Strain inhomogeneity was low in perfectly plastic material. It is also observed from these figures that the strain is more in perfectly plastic material than in strain hardening material. This is because the material does not deform fully in case of strain hardening material. The cross sectional views (Fig. 4, Fig. 5 and Fig. 6) also indicate the same phenomenon. These figures also indicate that the strain produced is lesser for larger channel angles [30].

Fig. 7 shows the variation of extrusion load as the workpiece is pressed. It indicates that the load decreases with increase in channel angle. More load is required for strain hardening material than perfectly plastic material.

Video 1 shows strain distribution during the extrusion for 105 degree channel angle strain hardening material. It is clear from the video that plastic deformation occurs at the plastic deformation zone and further no further change takes place in the workpiece.

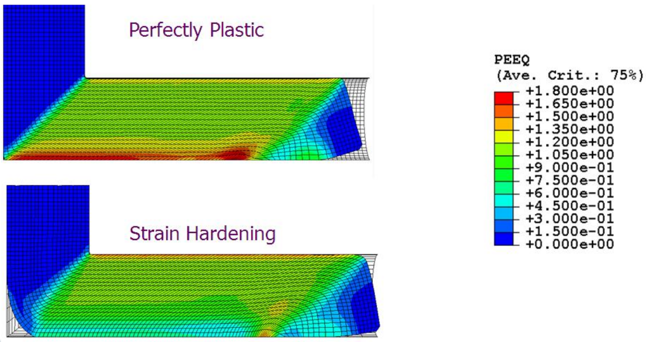

Fig. 1 Strain distribution along the workpiece of perfectly plastic and strain hardening material pressed by 90 degree channel angle

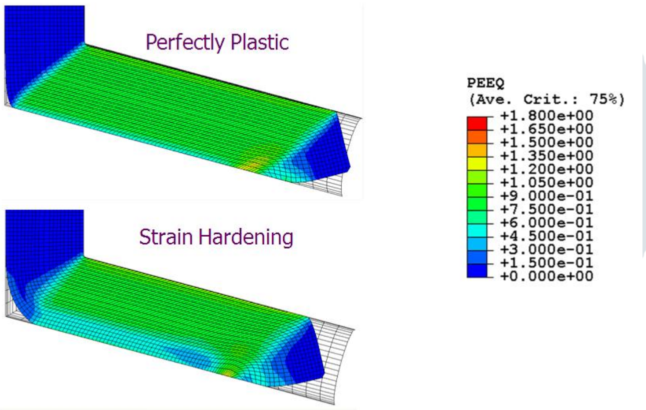

Fig. 2 Strain distribution along the workpiece of perfectly plastic and strain hardening material pressed by 105 degree channel angle

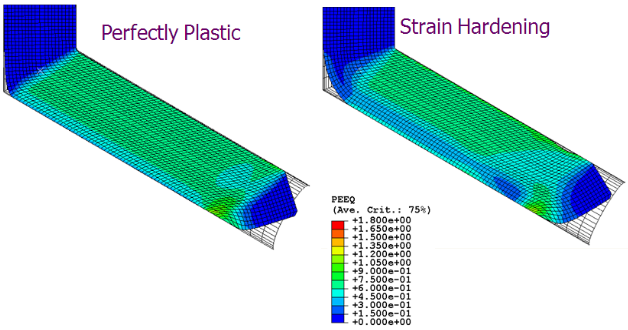

Fig. 3 Strain distribution along the workpiece of perfectly plastic and strain hardening material pressed by 120 degree channel angle

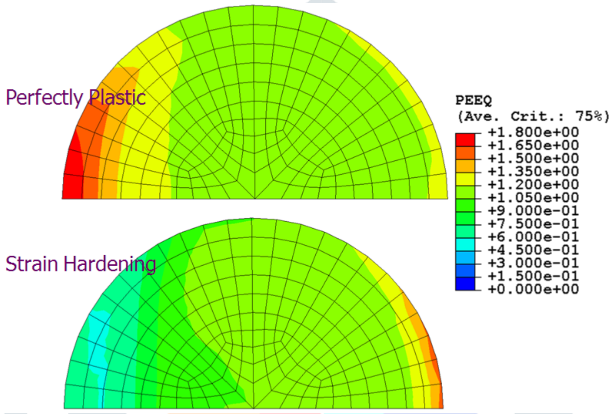

Fig. 4 Strain distribution across the workpiece of perfectly plastic and strain hardening material pressed by 90 degree channel angle

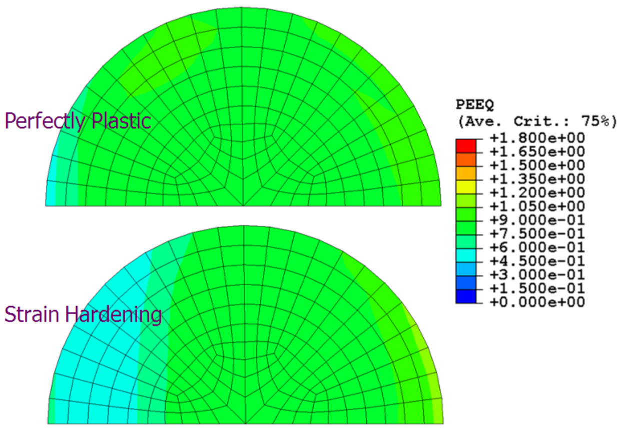

Fig. 5 Strain distribution across the workpiece of perfectly plastic and strain hardening material pressed by 105 degree channel angle

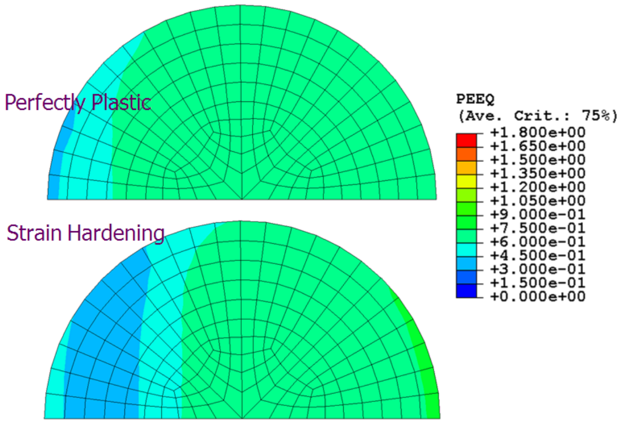

Fig. 6 Strain distribution across the workpiece of perfectly plastic and strain hardening material pressed by 120 degree channel angle

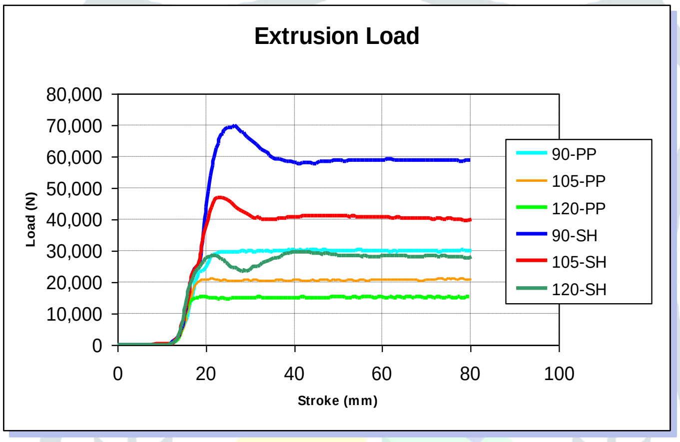

Fig. 7 Load required to press the workpiece

VI. CONCLUSION

Based on the 3D finite element analysis of ECAP with different material models following conclusions can be drawn:

- In the steady-state region, significant strain inhomogeneity exists across the workpiece
- Die corners are not completely filled due to strain hardening
- Strain inhomogeneity is lesser in perfectly plastic material than in strain hardening material
- Strain induced is more in perfectly plastic material than in strain hardening material
- Strain and load decrease with increasing die angle
- Die angle and material property have significant effect on variation in extrusion load

VII. REFERENCES

[1] Segal, V.M. (1995) Materials processing by simple shear. *Material Science and Engineering A*, 197, 157-164.

[2] Iwahashi, Y., Z. Horita, M. Nemoto and T.G. Langdon (1997) An investigation of microstructural evolution during equal channel angular pressing. *Acta Materialia*, 45, 4733-4741.

[3] Saito, Y., H. Utsunomiya, N. Tsuji and T. Sakai (1999) Novel ultra high straining process for bulk materials development of the accumulative roll bonding (ARB) process, *Acta Materialia*, 47, 579-583.

[4] Lee, J.W. and J.J. Park (2002) Numerical and experimental investigations of constrained groove pressing and rolling for grain refinement. *Journal of Materials Processing Technology*, 130, 208-213.

[5] Huang, J., Y.T. Zhu, J. David and T.C. Lowe (2004) Development of repetitive corrugation and straightening. *Material Science and Engineering A*, 371, 35-39.

[6] Zhu, Y.T., H. Jiang, J.Y. Huang and T.C. Lowe (2001) A new route to bulk nano-structured metals, *Metallurgical and Materials Transactions A*, 32, 1559-1562.

[7] Shin, D.H., J.J. Park, Y.S. Kim and K.T. Park (2002) Constrained groove pressing and its application to grain refinement of aluminium. *Material Science and Engineering A*, 328, 98-103.

[8] Segal, V.M., V.I. Reznikov, A.E. Drobyshevskii and V.I.Kopylov (1981) Plastic Metal Working by Simple Shear. *Izvestia Akademii nauk SSSR. Metally*, 1, 115-123.

[9] Valiev, R.Z., N.A. Krasilnikov and N.K. Tsenev (1991) Plastic deformation of alloys with sub-micron grained structure. *Material Science and Engineering A*, 137, 35-40.

[10] Valiev, R.Z., E.V. Kozlov, Ivanov, F. Yu, J. Lian, A.A. Nazarov and B. Baudelet (1994) Deformation behaviour of ultra-fine grained copper. *Acta Metallurgica et Materialia*, 42, 2467-2475.

[11] Korbel, A. and M. Richert (1985) Formation of shear bands during cyclic deformation of aluminium. *Acta Metallurgica*, 33, 1971-1978.

[12] Valiev, R.Z., R.K. Islamgaliev and I.V. Alexandrov (2000) Bulk nano-structured materials from severe plastic deformation. *Progress in Materials Science*, 45, 103-189.

[13] Saito, Y., H. Utsunomiya, N. Tsuji and T. Sakai (1999) Novel ultra high straining process for bulk materials development of the accumulative roll bonding (ARB) process, Acta Materialia, 47, 579-583.

[14] Chakkingal, U., A.B. Suriadi and P.F. Thomson (1998) Microstructure development during equal channel angular drawing of Al at room temperature. Scripta Materialia, 39, 677-684.

[15] Chakkingal, U., A.B. Suriadi and P.F. Thomson (1999) The development of microstructure and the influence of processing route during equal channel angular drawing of pure aluminium. Materials Science and Engineering A, 266, 241-249.

[16] Agnew, S.R. and J.R. Weertman (1998) Cyclic softening of ultra-fine grain copper. Materials Science and Engineering A, 244, 145-153.

[17] Iwahashi, Y., Z. Horita, M. Nemoto and T.G. Langdon (1997) An investigation of microstructural evolution during equal channel angular pressing. Acta Materialia, 45, 4733-4741.

[18] Sun, P.L., P.W. Kao and C.P. Chang (2000) Characteristics of sub-micron grained structure formed in aluminium by equal channel angular extrusion. Materials Science and Engineering A, 283, 82-85.

[19] Iwahashi, Y., Z. Horita, M. Nemoto and T.G. Langdon (1998) Factors influencing the equilibrium grain size in equal channel angular pressing: role of Mg additions to aluminium. *Metallurgical and Materials Transactions A, 29*, 2503-2510.

[20] Gholinia, A., P.B. Prangnell and M.V. Markushev (2000) The effect of strain path on the development of deformation structures in severely deformed aluminium alloys processed by ECAE. *Acta Materialia*, 48, 1115-1130.

[21] Berbon, P.B., M. Furukawa, Z. Horita, M. Nemoto and T.G. Langdon (1999) Influence of pressing speed on microstructural development in equal channel angular pressing. *Metallurgical and Material Transactions A*, 30, 1989-1997.

[22] Zienkiewicz O.C. and R.L. Taylor, The Finite Element Method. Vol. 2, Butterworth-Heinemann, Oxford, 2000.

[23] Belytschko, T., Wing Kam Liu and Brian Moran Nonlinear Finite Elements for Continua and Structures. John Wiley & Sons, USA, 2000.

[24] Sue, H.J., H. Dilan and C.K.Y. Li (1999) Simple shear plastic deformation behavior of polycarbonate plate due to the equal channel angular pressing process. I: Finite element methods modeling. Polymer Engineering and Science, 39 (12), 2505-2515.

[25] Semiatin, S.L., D.P. DeLo and E.B. Shell (2000) The effect of material properties and tooling design on deformation and fracture during equal channel angular extrusion. Acta Materialia, 48, 1841-1851.

[26] Lee, S.C., S.Y. Ha, K.T. Kim, S.M. Hwang, L.M. Huh and H.S. Chung (2004) Finite element analysis for deformation behavior of an aluminum alloy composite containing SiC particles and porosities during ECAP. Materials Science and Engineering A, 371 (1-2), 306-312.

[27] Zairi, F., B. Aour, J.M. Gloaguen, M. Nait-Abdelaziz and J.M. Lefebvre (2006) Numerical modeling of elastic-viscoplastic equal channel angular pressing process of a polymer. Computational Materials Science, 38 (1), 202-216.

[28] Aour, B., F. Zairi, J.M. Gloaguen, M. Nait-Abdelaziz and J.M. Lefebvre (2006) Numerical investigation on equal channel angular pressing process of polymers. Computational Materials Science, 37 (4), 491-506.

[29] Figueiredo, R.B., M.T.P. Aguilar and P.R. Cetlin (2006) Finite element modeling of plastic instability during ECAP processing of flow-softening materials. Materials Science and Engineering A, 430 (1-2), 179-184.

[30] Patil Basavaraj V, Uday Chakkingal, T. S. Prasanna Kumar, "Study of channel angle influence on material flow and strain inhomogeneity in equal channel angular pressing using 3D finite element simulation", Journal of Material Processing Technology, 2009, 209 (1), pp 89

*****